RAPID COMMUNICATIONS

PHYSICAL REVIEW C VOLUME 39, NUMBER 2 FEBRUARY 1989

Absorptive effects in $K^+\Lambda$ photoproduction on nucleons and nuclei

H. Tanabe, M. Kohno, and C. Bennhold
Institut für Kernphysik, Johannes Gutenberg-Universität Mainz, D-6500 Mainz, West Germany
(Received 14 November 1988)

Incorporating final-state correlation effects, we have reinvestigated the $\gamma^1\text{H} \rightarrow K^+\Lambda$ elementary process. Our model not only resolves the persisting trouble of the small $KN\Lambda$ coupling constant, but also yields agreement with cross-section data at higher energies. Using our amplitudes, we calculate angular distributions for the reaction $^{16}\text{O}(\gamma,K^+)^{16}_{\Lambda}\text{N}$. While the forward cross section increases with increasing energy, the total cross section is almost constant from $E_\gamma = 1.2$ through 2 GeV, suggesting that rather low photon energies hold promise for exploration of hypernuclear excitations.

There has been an increasing interest in the production of hypernuclei via electromagnetic reactions,[1-3] such as $^1\text{H}(\gamma,K^+)\Lambda$. It is the advantage of the photoproduction process that both the photon and the K^+, with its mean-free path of about 7 fm in the nuclear medium, interact rather weakly with the nucleus so that the reaction can occur deep in the nuclear interior as compared to K^- and $\pi^\pm$ which are strongly absorbed and thus confine their reaction to the nuclear periphery.

To explore these hypernuclear formation reactions, however, knowledge of the basic elementary process is essential. Despite a number of investigations (Refs. 4 and 5, and references therein), an understanding of the kaon photoproduction process remains elusive. One persisting trouble[2,6] is that the $KN\Lambda$ coupling constant deduced from most analyses of $^1\text{H}(\gamma,K^+)\Lambda$ is about half the standard value: namely, $g^2_{KN\Lambda}/4\pi \sim 4$ has been deduced[4,5] instead of $g^2_{KN\Lambda}/4\pi \sim 14$,[7] although a recent study[8] shows that the standard value can be recovered by including an additional t-channel resonance.

Another problem consists of the energy region to be considered. Since the momentum transfer decreases for 0° kaons with increasing energy, higher energies of $E_\gamma = 1.5$–2.0 GeV have been recommended for the actual formation of hypernuclei. However, as depicted in Fig. 1, previous models, which have been focused on the process below $E_\gamma = 1.4$ GeV, cannot reproduce the $\gamma^1\text{H} \rightarrow K^+\Lambda$ total cross-section data above 1.5 GeV. Thus, it is desirable to develop more realistic models, covering the energy range up to ~ 2 GeV, and to examine their consequences for hypernuclear excitations. Since new experimental data on hypernuclear electromagnetic production are expected in the future, we reinvestigate in this study the $K^+\Lambda$ photoproduction process, considering Born terms and various resonance contributions.

Almost all parametrizations of the kaon photoproduction operator for use in hypernuclear formation studies have so far ignored the effects of $K^+\Lambda$ final-state correlations, which ought to be very strong even at threshold since many other channels are open. On the other hand, more careful analyses have been done for hadronic reactions such as $K^\pm N$ scattering.[7] Therefore, the standard value for $g_{KN\Lambda}$ deduced from these processes is regarded as more reliable. The small $g_{KN\Lambda}$ in the analysis of $^1\text{H}(\gamma,K^+)\Lambda$, in our opinion, simply implies the importance of taking into account $K^+\Lambda$ absorptive effects.

It may be argued that the small $KN\Lambda$ coupling constant in the previous analyses[4,5] should be regarded as an effective one, simulating effects of the final-state interaction. However, correlation effects are angular-momentum dependent, and can modify the partial wave structure of the kaon photoproduction amplitude. Such effects are not represented merely by rescaling the coupling constant. Since the protons and Λ are in certain orbits and their angular-momentum coupling is specified in hypernuclear excitations, the absorptive corrections are expected to provide nontrivial effects on the hypernuclear formation cross section.

The basic Born amplitudes from kaon-baryon pseudoscalar couplings and their decomposition into multipoles have been established.[4,5] In the analysis presented here, the absorptive effects are simulated by multiplying each multipole of the Born amplitudes with a reduction factor of the form

$$\{1+\exp[(R-l/q)/a]\}^{-1}, \qquad (1)$$

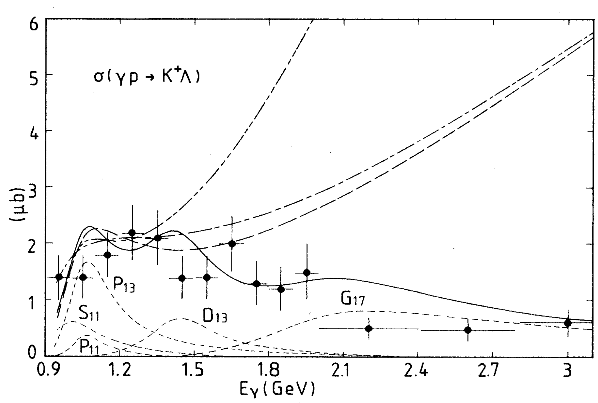

FIG. 1. Total $\gamma^1\text{H} \rightarrow K^+\Lambda$ cross section as a function of laboratory photon energy. The solid curve represents our result, for which several resonance contributions are also shown by dashed curves. The long dashed, dash-dotted, and dash-two-dotted curves are from the model 1 of Ref. 5, model 2 of Ref. 4, and model 2 of Ref. 8, respectively. The data are from Ref. 11.

where l and q denote the partial wave and momentum in the final channel, and a and R are parameters to be adjusted. The underlying picture[9] of this factor is that the partial waves inside a region of radius R and diffuseness a are strongly suppressed by absorptive processes. The black-disk nature of the absorptive region is inferred from the fact that in the SU(3) related $K^{-}\,{}^{1}\mathrm{H}$ scattering data at higher energies[10] the absorptive cross section is as large as the elastic one.

The description of the process has been improved by introducing various resonances.[4,5,11,12] In our study, we take into account five resonances; $S_{11}(1640-i75)$, $P_{11}(1690-i40)$, $P_{13}(1680-i60)$, $D_{13}(1880-i80)$, and $G_{17}(2100-i200)$, which have a nonnegligible branching ratio to the $K\Lambda$ channel. The $P_{11}(1470-i100)$ resonance is omitted because of its weak coupling to the $K\Lambda$ channel.[13] The importance of the G_{17} resonance, on the other hand, is suggested by enhancement observed in the $\pi^{-}\,{}^{1}\mathrm{H}\rightarrow K^{0}\Lambda$ total cross section.[14] The resonance amplitudes are assumed to have the Breit-Wigner form

$$E_{l\pm},\, M_{l\pm}=\frac{1}{[q_0k_0j_\gamma(j_\gamma+1)]^{1/2}}\left[\frac{v_l(qR)}{v_l(q_0R)}\right]^{1/2}\times\frac{m_0\Gamma\sqrt{x_\gamma x_K}}{m_0^2-s-im_0\Gamma}e^{i\theta}, \tag{2}$$

where $j_\gamma=l\pm1$ for an electric multipole amplitude $E_{l\pm}$ and $j_\gamma=l$ for a magnetic multipole amplitude $M_{l\pm}$. Here, s is the square of the total center of momentum energy, k_0 and q_0 are on-resonance momenta of the photon and kaon, respectively, $m_0-i\Gamma/2$ is the pole position of the resonant state, and θ is the phase angle. The $v_l(qR)$ is a barrier penetration factor,[15] in which the interaction radius parameter R is set to be the same as the radius R of Eq. (1). The factors x_γ and x_K represent the branching ratios into $\gamma\,{}^{1}\mathrm{H}$ and $K^{+}\Lambda$ states from the resonance, respectively.

In our study, the coupling constants for the Born amplitudes are not included in the fitting procedure. The $KN\Lambda$ and $KN\Sigma$ coupling constants are set to be the standard values:[7] $g_{KN\Lambda}/\sqrt{4\pi}=-3.73$ and $g_{KN\Sigma}/\sqrt{4\pi}=1.82$. The value for $g_{KN\Sigma}$ has been varying in the literature. This rather large $g_{KN\Sigma}$ is in agreement with the most recent determination.[16] The experimental values are taken for the magnetic moments: $\mu_p=2.79\ \mu_N$, $\mu_\Lambda=-0.613\ \mu_N$ (Ref. 10) and $\mu_T=-1.59\ \mu_N$.[17] Two coupling constants of the K^*,

$$G_V/4\pi\equiv g_{K^*K\gamma}\cdot g^{V}_{K^*N\Lambda}/4\pi=-0.0913$$

and

$$G_T/4\pi\equiv g_{K^*K\gamma}\cdot g^{T}_{K^*N\Lambda}/4\pi=-0.371\,,$$

are estimated[18] from the known value for $g_{K^*K\gamma}$ and by assuming the SU(3) relation between the $g^{V,T}_{K^*N\Lambda}$ and $g^{V,T}_{\rho NN}$, of which the latter is known approximately. The two parameters in Eq. (1) and resonance parameters are adjusted so as to give a best χ^2 fit to all available data[11,19,20] up to 3 GeV. The resulting geometry, $R=0.748$ fm and $a=0.0974$ fm, is reasonable in view of the above physical interpretation. The resonance parameters in our fit are tabulated in Table I, where they compare favorably to the values estimated from other independent sources, such as pion photoproduction, the $\pi^{-}\,{}^{1}\mathrm{H}\rightarrow K^{0}\Lambda$ reaction and πN elastic scattering data.[10] The χ^2 per data point in our model is 3.64, which is comparable with the χ^2 of the models of Refs. 4, 5, and 8. Note that in these references only the data below $E_\gamma=1.4$ GeV were considered.

Figure 1 compares several theoretical calculations with $\gamma\,{}^{1}\mathrm{H}\rightarrow K^{+}\Lambda$ total cross-section data. The solid curve shows our result, while the other curves are obtained from various models that did not include absorptive corrections. As mentioned before, all other models fail to reproduce the trend of the experimental data above $E_\gamma\sim1.5$ GeV. As expected, the Born term contributions (Thom's model) rise monotonically with increasing energy. To suppress these large contributions, it is essential to incorporate absorptive effects. When the final-state interaction effects are included, the Born term contributions are not large enough to fit the data especially at low energies. Here the resonances play an important role. At higher energies around 2 GeV, certain resonance contributions, represented by the G_{17} in our model, are decisive in reproducing the differential cross-section data at 25° from Ref. 20.

Now we consider the hypernuclear formation cross section in a nonrelativistic framework, assuming plane waves for the outgoing kaons. Using the impulse approximation, we evaluate the single-particle matrix elements in momentum space[3]

$$\langle f,K^{+}|t|i,\gamma\rangle=\int d\mathbf{p}\,d\mathbf{p}'\,\delta(\mathbf{k}+\mathbf{p}-\mathbf{q}-\mathbf{p}')\times\psi_f^{*}(\mathbf{p}')t_{\gamma p\rightarrow K\Lambda}(\mathbf{k},\mathbf{p},\mathbf{q},\mathbf{p}')\psi_i(\mathbf{p})\,, \tag{3}$$

where ψ_f and ψ_i are the Λ and proton wave functions, respectively, and the momenta of the photon, proton, kaon, and Λ are denoted by $\mathbf{k}$, $\mathbf{p}$, $\mathbf{q}$, and $\mathbf{p}'$, respectively. At each value of the proton momentum $\mathbf{p}$, the amplitude $t_{\gamma p\rightarrow K\Lambda}$ in Eq. (3) is identified with that in the respective $\gamma\,{}^{1}\mathrm{H}$ center-of-momentum frame. The single-particle wave functions are provided by solving the Schrödinger equation with a standard Woods-Saxon potential.

Figure 2 shows differential cross sections of 1^{-} and 0^{-} transitions of the $({}_{\Lambda}s_{1/2},p_{1/2}^{-1})$ ground-state hypernuclear formation on ${}^{16}\mathrm{O}$ at $E_\gamma=1.3$ GeV, using four models as in Fig. 1. At forward angles the structure of the kaon pho-

TABLE I. Resonance states and their parameters. Reference values from other sources are given in the parentheses.

Resonance		$m_0-i\Gamma/2$ (MeV)	$\sqrt{x_\gamma x_K}$ (10^{-3})	θ (deg.)
S_{11}	E_{0+}	$1640-i75$	8.13	−107.8
			(7.9 ± 2.8)	(−75 ± 25)
P_{11}	M_{1-}	$1690-i40$	−7.21	176.3
			(1.6 ± 5.3)	(175 ± 35)
P_{13}	E_{1+}	$1680-i60$	9.52	−103.4
			(9.1 ± 6.3)	(−160 ± 30)
	M_{1+}		3.18	
			(−0.5 ± 4.3)	
D_{13}	E_{2-}	$1880-i80$	4.09	−35.9
	M_{2-}		−7.09	
G_{17}	E_{4-}	$2100-i200$	2.04	−27.5
	M_{4-}		−5.78	

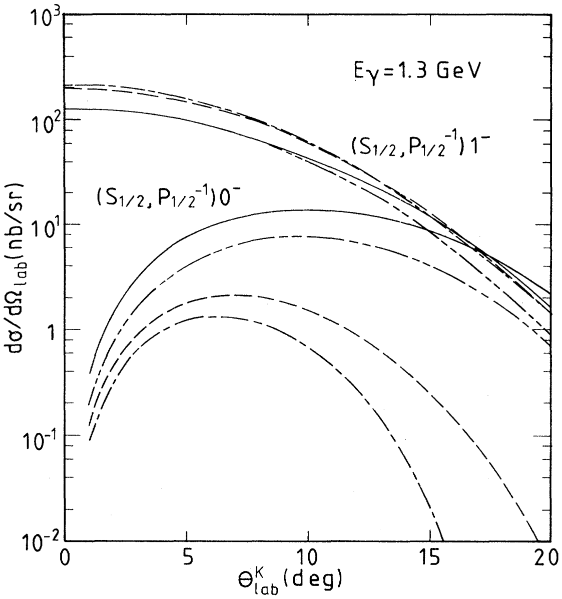

FIG. 2. Differential cross sections of the hypernuclear formation on ^{16}O. The curves are as in Fig. 1.

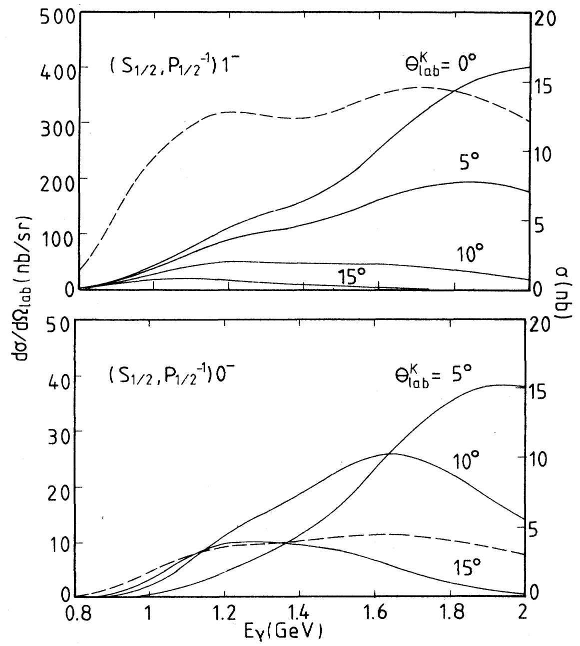

FIG. 3. Energy dependence of the differential cross sections of the hypernuclear formation on ^{16}O, calculated by our model. An angle-integrated cross section is also shown by a dashed curve for each transition.

toproduction operator simplifies, because all terms other than leading $\sigma\cdot\epsilon$ vanish for 0° kaons, where ϵ is the photon polarization vector. In the present case of the p to s transition, the matrix element from the $\sigma\cdot\epsilon$ term is, in the plane-wave approximation for kaons, proportional to $(\mathbf{p}\times\epsilon)^{(J)}$. Thus, at forward angles where the contributions from the proton momentum $\mathbf{p}\|\mathbf{k}$ dominate, the $J=0$ transition is kinematically suppressed, and the dominant reaction proceeds through the 1^- state. Because the leading $\sigma\cdot\epsilon$ term should be similar in each model which fits the data of the elementary process below $E_\gamma=1.4$ GeV, the model dependence of this dominant 1^- excitation is rather small. On the other hand, the 0^- transition is sensitive to the details of the spin and partial-wave structure of the elementary amplitudes. Our model gives much larger cross sections for this transition, compared with the other three models.

In Fig. 3 we show the energy dependence of the total cross sections and differential cross sections at $\theta_K^{\rm lab}=0°$, 5°, 10°, and 15° both for the 1^- and 0^- transitions. The cross section for 0° kaons in hypernuclear formation increases with increasing energy. This is because the decreasing momentum transfer makes nuclear matrix elements larger, while the elementary cross sections at forward angles for $E_\gamma=1.5\sim2$ GeV remain as large as those at $E_\gamma=1.2\sim1.5$ GeV, as the data[20] at $\theta_K=25°$ indicate, in spite of the decrease of the total $\gamma\,^1{\rm H}\rightarrow K^+\Lambda$ cross section. Away from the forward direction, the momentum transfer increases with rising energy. Reflecting this property, the differential cross section at finite angles reaches its maximum below $E_\gamma=2$ GeV.

In the literature,[1-3] the energy region around $E_\gamma=2$ GeV has been cited as optimal for hypernuclear study. The energy dependence of the forward cross section from our model, in Fig. 3, clearly supports this estimate. On the other hand, we also notice that the total cross section of the 1^- transition is almost constant from $E_\gamma=1.2$ through 2 GeV. This suggests that for the experiments using a detector covering wide solid angles it is not necessary to go to higher energies where the energy resolution generally becomes worse. Since the 0^- transition is suppressed at 0°, this differential cross section has a maximum at finite angles. If the 0^- strength is large enough, the experimentally observed angular distribution should show some structure, even though the two states may not be energetically separated. Figure 3 indicates that there might be hope[2] of separating the two contributions around $E_\gamma=1.6$ GeV, where the relative strength of the 0^- to 1^- is seen to be increased.

In the present calculations, kaons are approximated by plane waves for simplicitly as a first application of our elementary amplitudes. Kaon distortion effects have been known[2,3] to reduce the hypernuclear cross sections by 10–30%, but not to change their qualitative character. These distortion effects and a more elaborate treatment for the Lorentz transformation of the absorptive factors will be studied in a future work.

In summary, we have shown that the inclusion of $K^+\Lambda$ final-state absorptive effects is essential for describing the kaon photoproduction process up to 2 GeV. Not only can the standard value for $g_{KN\Lambda}$ be maintained, but also realistic operators for energies above $E_\gamma\sim1.5$ GeV are obtained. Using our amplitudes, we have explicitly calculated differential cross sections of the $({}_\Lambda s_{1/2},p_{1/2}^{-1})$ transition in $^{16}{\rm O}(\gamma,K^+)^{16}_{\Lambda}{\rm N}$. Based on these results, we have remarked that incident energies below $E_\gamma=1.6$ GeV are also promising for hypernuclear studies.

This work was supported by the Deutsche Forschungsgemeinschaft Grant No. SFB201.

[1]A. M. Bernstein, T. W. Donnelly, and G. N. Epstein, Nucl. Phys. **A358**, 195c (1981); S. R. Cotanch and S. S. Hsiao, *ibid.* **A450**, 419c (1986); J. Cohen, in *Proceedings of the Continuous Electron Beam Accelerator Facility (CEBAF) Summer Workshop, Newport News, Virginia, 1986,* edited by V. Burkert *et al.* (Continuous Electron Beam Accelerator Facility, Newport News, VA, 1987), p. 305.

[2]A. S. Rosenthal *et al.*, Ann. Phys. (N.Y.) **184**, 33 (1988).

[3]C. Bennhold and L. E. Wright, Phys. Lett. **191**, 11 (1987); Prog. Part. Nucl. Phys. **20**, 377 (1988).

[4]H. Thom, Phys. Rev. **151**, 1322 (1966).

[5]R. A. Adelseck, C. Bennhold, and L. E. Wright, Phys. Rev. C **32**, 1681 (1985).

[6]J. Cohen, Phys. Lett. **192**, 291 (1987).

[7]A. D. Martin, Nucl. Phys. B **179**, 33 (1981).

[8]R. A. Adelseck and L. E. Wright, Phys. Rev. C **38**, 1965 (1988).

[9]K. Gottfried and J. D. Jackson, Nuovo Cimento **34**, 735 (1964).

[10]Particle Data Group, Phys. Lett. **170B**, 1 (1986).

[11]W. Schorsch, J. Tietge, and W. Weilnböck, Nucl. Phys. **B25**, 179 (1970).

[12]S. R. Deans *et al.*, Phys. Rev. D **6**, 1906 (1972).

[13]F. Wagner and C. Lovelace, Nucl. Phys. **B25**, 411 (1971).

[14]V. Flaminio *et al.*, European Organization for Nuclear Research-Hadron Electron Ring Accelerator, Report No. 83-01, 1983 (unpublished).

[15]J. M. Blatt and V. F. Weisskopf, *Theoretical Nuclear Physics* (Wiley, New York, 1952).

[16]J. Antolin, Phys. Rev. D **35**, 122 (1987).

[17]P. C. Petersen *et al.*, Phys. Rev. Lett. **57**, 949 (1986).

[18]R. L. Workman and H. W. Fearing, Phys. Rev. D **37**, 3117 (1988).

[19]H. Genzel, P. Joos, and W. Pfeil, *Photoproduction of Elementary Particles,* Landolt-Börnstein, Numerical Data and Functional Relationships in Science and Technology, Group I, Vol. 8 (Springer-Verlag, Berlin, 1973).

[20]P. Feller *et al.*, Nucl. Phys. B **39**, 413 (1972).